Electronic structure reconstruction by trimer formation in CsW_2O_6 studied by x-ray photoelectron spectroscopy

R. Nakamura,[1] D. Takegami,[2] A. Melendez-Sans,[2] L. H. Tjeng,[2] M. Okawa,[1] T. Miyoshino,[1] N. L. Saini,[3] M. Kitamura,[4] D. Shiga,[5] H. Kumigashira,[5] M. Yoshimura,[6] K.-D. Tsuei,[6] Y. Okamoto,[7] and T. Mizokawa[1]

[1]*Department of Applied Physics, Waseda University, Shinjuku, Tokyo 169-8555, Japan*
[2]*Max Planck Institute for Chemical Physics of Solids, 01187 Dresden, Germany*
[3]*Department of Physics, University of Roma "La Sapienza" Piazalle Aldo Moro 2, 00185 Roma, Italy*
[4]*Institute of Materials Structure Science, High Energy Accelerator Research Organization (KEK), Tsukuba, Ibaraki 305-0801, Japan*
[5]*Institute of Multidisciplinary Research for Advanced Materials (IMRAM), Tohoku University, Sendai 980-8577, Japan*
[6]*National Synchrotron Radiation Research Center, 30076 Hsinchu, Taiwan*
[7]*Institute for Solid State Physics, University of Tokyo, Kashiwa Chiba 277-8581, Japan*

(Received 14 September 2022; accepted 14 October 2022; published 2 November 2022)

We have studied the electronic structure of CsW_2O_6 across its metal-insulator transition by means of hard/soft x-ray photoelectron spectroscopy. In the high-temperature metallic phase, the W 5*d* band exhibits a clear Fermi edge. The W $4f_{7/2}$ and $4f_{5/2}$ core-level peaks are accompanied by shoulders on their lower binding energy side. The shoulder and main peaks, respectively, are attributed to the well- and poorly screened final states where the screening is due to the W 5*d* electronic states in the vicinity of the chemical potential. In going from 300 to 180 K (across the metal-insulator transition), a band gap of about 0.2 eV is created at the Fermi level. The origin of the band gap can be assigned to the trimerization of the W sites. The W 4*f* and 5*d* spectra exclude the possibility of charge disproportionation and suggest moderate electronic correlation effects.

DOI: 10.1103/PhysRevB.106.195104

I. INTRODUCTION

In transition-metal compounds with octahedral coordination, the transition-metal *d* orbitals are split into doubly degenerate e_g orbitals and triply degenerate t_{2g} orbitals. When the low-lying t_{2g} orbitals are partially occupied by electrons, the transition-metal compounds are known as t_{2g} electron systems. Several t_{2g} electron systems on a pyrochlore lattice (such as $CuIr_2S_4$ and $MgTi_2O_4$ with spinel structures) exhibit interesting metal-insulator transitions [1,2]. Their insulating phases are stabilized by multimers of transition-metal ions [3,4]. The band-gap opening and the multimer formation can be described by the orbitally induced Peierls mechanism [5].

Among the t_{2g} electron systems on a pyrochlore lattice, CsW_2O_6 with a β-pyrochlore structure exhibits a unique metal-insulator transition around 215 K which is accompanied by formation of W trimers [6–8]. The pyrochlore structure is shown in Fig. 1 which is created by VESTA [9]. Interestingly, Okamoto *et al.* revealed that the crystal symmetry of the insulating phase just below the transition is still cubic although the tetrahedron of W sites in the pyrochlore lattice is strongly distorted by the trimer formation [8]. The trimers would be formed by W^{5+} sites with t_{2g}^1 configuration. However, since the formal valence of W is +5.5 in CsW_2O_6, it is difficult to construct such W^{5+} trimers keeping the cubic symmetry. Instead, it has been proposed that the trimers are formed by $W^{5.33+}$ sites. In this scenario, each W trimer has two W 5*d* t_{2g} electrons.

The metal-insulator transition and the trimerization in CsW_2O_6 have been attracting great interest from also the theory community. Streltsov *et al.* proposed that the metal-insulator transition is due to a spin-orbital induced Peierls mechanism [10]. More recently, Nakai and Hotta proposed a new mechanism due to a flat band created by the pyrochlore lattice geometry and the spin-orbit interaction [11]. In addition, the electron-electron interaction may play some roles in the exotic phase transition. In this context, it is highly important to investigate the electronic structure of CsW_2O_6 by means of photoelectron spectroscopy. So far, one photoelectron spectroscopy study on epitaxially grown CsW_2O_6 thin films has been reported [12]. In that study, the main and shoulder peaks of W 4*f* observed in the insulating phase are assigned to W^{6+} and W^{5+} although their intensity ratio is very different from the expected ratio W^{6+}:W^{5+} = 1:1. The existence of W^{6+} and W^{5+} is not consistent with the proposed theoretical models. Also large changes were observed for, in particular, the Cs-derived states across the metal-insulator transition.

In the present paper, we report hard/soft x-ray photoelectron spectroscopy (HAXPES/SOXPES) of polycrystalline CsW_2O_6 with the objective to obtain spectra that are representative of the bulk material. Across the metal-insulator transition, we observed modest and mostly energy-shift-like changes in all spectral sections. We came to a different interpretation of the spectra and discussed the results vis-à-vis the existing theoretical models.

II. EXPERIMENT

Polycrystalline samples of CsW_2O_6 were synthesized as reported in the literature [8,13]. HAXPES measurements were

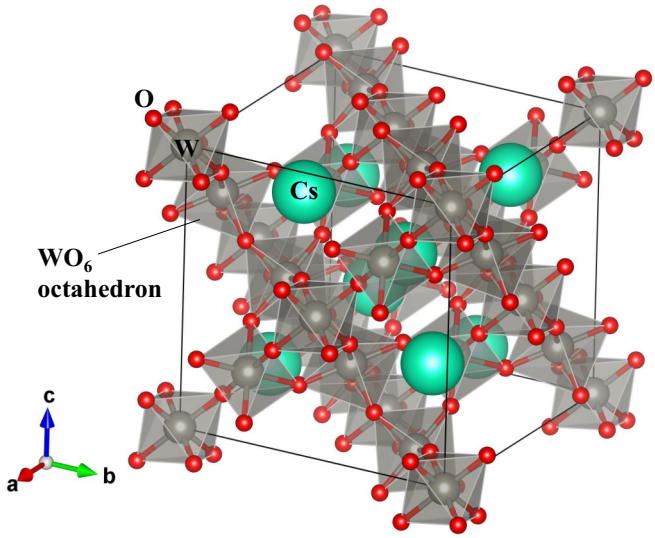

FIG. 1. Crystal structure of β-pyrochlore CsW_2O_6 illustrated by using VESTA [9]. The W sites form a pyrochlore lattice.

performed at the Max-Planck-NSRRC HAXPES end station [14], Taiwan undulator beam line BL12XU of SPring-8 with 6.5-keV photon energy. The probing depth is determined by the inelastic mean free path of the photoelectrons (with the kinetic energy of 5.5–6.5 keV) which is estimated to be about 4 to 5 nm in the universal curve [15] and is about 10 nm for various inorganic compounds in the recent calculation [16]. The x-ray incidence angle was 15° with respect to the sample surface, and the photoelectron detection angle was 15° off from the surface normal of the sample and parallel to the E vector of the x ray. The polycrystalline samples were fractured under ultrahigh vacuum of 10^{-6} Pa at 300 K in order to obtain clean sample surfaces. The measurements were performed at 300 and 180 K. The total energy resolution was about 300 meV. SOXPES measurements were performed at the MUSASHI end station, BL-2A of Photon Factory with 1200-eV photon energy. The inelastic mean free path of the photoelectrons (with the kinetic energy of 0.7–1.2 keV) is about 1 to 2 nm [15,16]. Photoionization cross section tends to be larger in SOXPES than in HAXPES [17]. The polycrystalline samples were fractured under ultrahigh vacuum of 10^{-8} Pa at 240 K and were measured between 240 and 190 K. The total energy resolution was about 200 meV. The binding energy of all spectra was calibrated using the Fermi edge of Au.

III. RESULTS AND DISCUSSION

The O 1s, Cs 4d, and Cs 3d HAXPES spectra taken at 300 and 180 K are displayed in Fig. 2. The O 1s and Cs $4d_{3/2}/4d_{1/2}$ peaks are shifted by about 0.1 eV toward the higher binding energy side in going from 300 to 180 K. This energy shift is quite consistent with the band-gap opening across the metal-insulator transition. The Cs $4d_{5/2}$, $4d_{3/2}$, $3d_{5/2}$, and $3d_{3/2}$ peaks have a single component and not two alike in the previous study [12]. In the present HAXPES measurements on the bulk of CsW_2O_6, the electronic state of Cs is very homogeneous and does not show relevant spectral

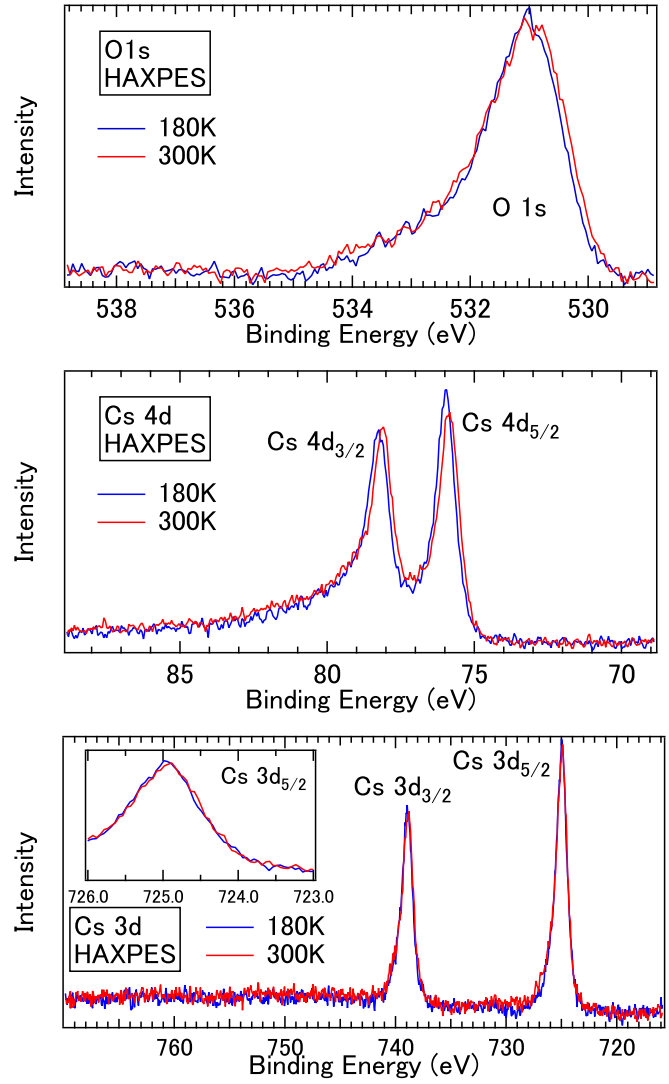

FIG. 2. O 1s (top), Cs 4d (middle), and Cs 3d (bottom) HAXPES spectra of CsW_2O_6 taken at 300 and 180 K.

change in going from 300 to 180 K. These results indicate that Cs is not taking an active role for the metal-insulator transition.

Figure 3 shows O 1s and Cs 3d SOXPES spectra taken at 240, 230, 220, 210, 200, and 190 K. The O 1s and Cs 3d peaks gradually shift toward the higher binding energy with cooling. This binding energy shift is basically consistent with the HAXPES results. The O 1s peak is accompanied by the tail on the higher binding energy side. The tail can be assigned to oxygen contamination in the surface region.

Figure 4 shows W 4f and W 5p HAXPES spectra taken at 300 and 180 K. The W $5p_{1/2}$ peak at about 52 eV is highly asymmetric with the tail on the lower binding energy side. The lower binding energy tail of the W $5p_{3/2}$ peak overlaps with the W $4f_{5/2}$ peak. The W $4f_{7/2}$ peak is also asymmetric with the shoulder peak on the lower binding energy side. In the previous study [12], the W $4f_{7/2}$ spectrum at 300 K was fitted by only a single component, and the shoulder peak was observed at 120 and 40 K below the metal-insulator transition. The shoulder and main peaks were assigned to W^{5+} and W^{6+},

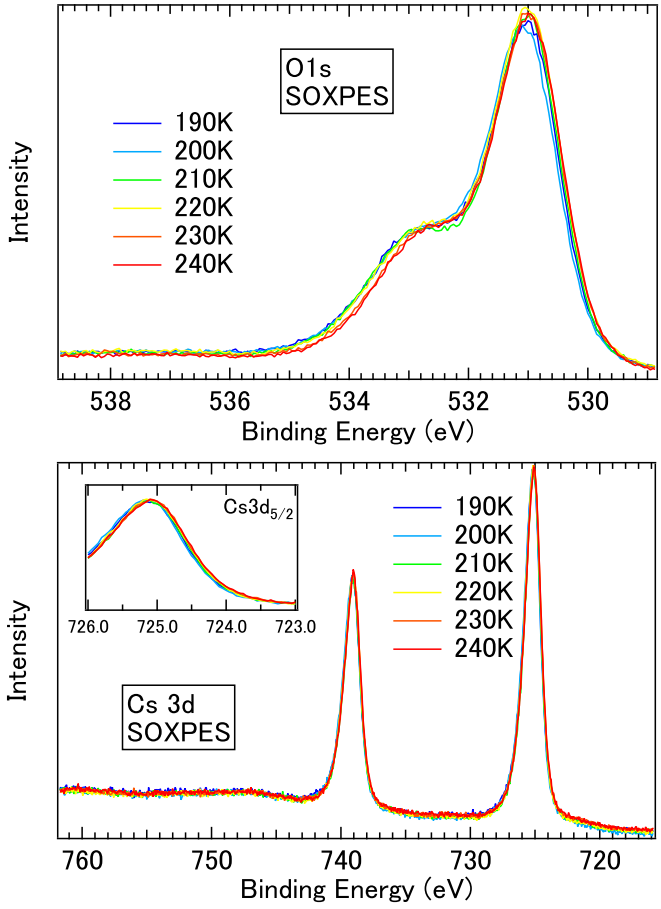

FIG. 3. O 1*s* (top) and Cs 3*d* (bottom) SOXPES spectra of CsW_2O_6 taken at 240, 230, 220, 210, 200, and 190 K.

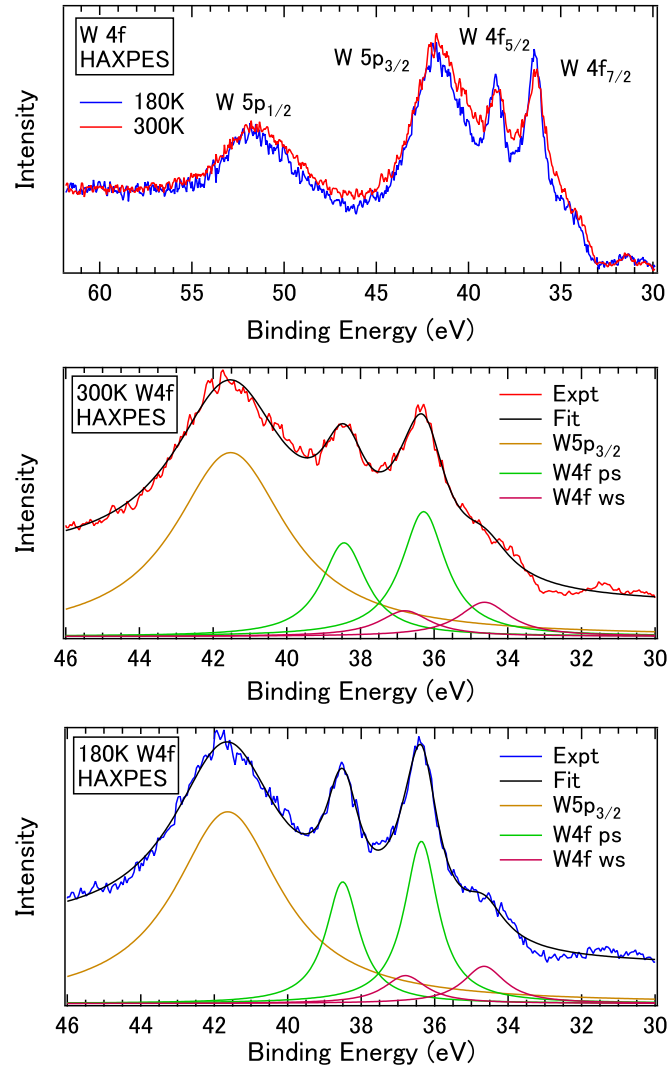

FIG. 4. W 4*f* HAXPES spectra of CsW_2O_6 taken at 300 and 180 K (top). The spectra at 300 K (middle) and 180 K (bottom) are fitted to Lorentzian functions. The solid curves represent the fitted results and the Lorentzian components.

respectively, although the intensity ratio is very different from the expected value of W^{5+}:$W^{6+} = 1{:}1$ [12]. In the present paper as shown in Fig. 4, the W $4f_{7/2}$ spectrum at 300 K already exhibits the main and shoulder peaks. Therefore, instead of the W^{5+} (or $W^{5.33+}$) contribution, the shoulder peak can be assigned to screening effect by the W 5*d* conduction electrons. The main and shoulder peaks corresponding to the poorly and well-screened peaks, respectively, as commonly seen in barely metallic or small gap 4*d* transition-metal oxides including $Ca_{2-x}Sr_xRuO_4$ [18–21], $CaCu_3Ru_4O_{12}$ [22–24], $LiRh_2O_4$ [25], and $Ba_{3-x}Sr_xNb_5O_{15}$ [26,27].

On the other hand, in mixed valence 3*d* transition-metal oxides, such as Fe_3O_4 and $BaV_{10}O_{15}$, transition-metal 2*p* core-level spectra often exhibit two components corresponding to different valence states even without static charge disproportion or charge ordering [28–31]. Here for CsW_2O_6, assuming strong trimer fluctuations or charge fluctuations in the metallic phase similar to $BaV_{10}O_{15}$ or Fe_3O_4, one may try to assign the main and shoulder peaks at 300 K to different valence states. In the proposed charge disproportionation scenarios, the shoulder peak at the lower binding energy side should be assigned to W^{5+} (W^{5+}:$W^{6+} = 1{:}1$) or $W^{5.33+}$ ($W^{5.33+}$:$W^{6+} = 3{:}1$) providing the intensity ratio between the shoulder and the main peaks of 1:1 or 3:1. However, the intensity of the shoulder peak is much smaller than that of the main peak, and, therefore, the charge disproportionation scenarios can be excluded. In another charge disproportionation scenario, the W trimers are formed by $W^{5.67+}$, and the remaining site is W^{5+}. In this scenario, the shoulder peak can be assigned to W^{5+} (W^{5+}:$W^{5.67+} = 1{:}3$) and the intensity ratio between the shoulder and the main peaks becomes 1:3, which would be consistent with the observation. However, the W^{5+} site and the trimers with one t_{2g} electron should have localized spins which are inconsistent with the nonmagnetic ground state [8]. Both above and below the transition temperature, the W 4*f* HAXPES spectrum is not compatible with any of the charge disproportionation scenarios. This situation of CsW_2O_6 is in sharp contrast to that of $LiRh_2O_4$ [25] or $CuIr_2S_4$ [32] in which the core-level spectrum is consistent with the Rh^{3+}/Rh^{4+} or Ir^{3+}/Ir^{4+} charge disproportionation.

Let us continue the argument on the shoulder peak based on the scenario of the screening effect. The spectral weight of the shoulder peak decreases in going from 300 to 180 K, indicating reduction of the screening effect in the insulating

phase. Such a shoulder peak in core-level spectra is commonly observed in various 4*d* transition-metal oxides with moderately correlated 4*d* electrons, such as $Ca_{2-x}Sr_xRuO_4$ [18–21], $CaCu_3Ru_4O_{12}$ [22–24], and $Ba_{3-x}Sr_xNb_5O_{15}$ [26,27]. However, it has never been reported in 5*d*-electron systems where the electronic correlation is much weaker than that in the 4*d*-electron systems. Most probably, the electronic correlation in the W 5*d* band is enhanced in CsW_2O_6 due to the pyrochlore lattice geometry and the spin-orbit interaction as pointed out by Nakai and Hotta [11]. The shoulder peak remains in the insulating phase indicating itinerant character of the W 5*d* electrons, although they are moderately correlated. The main and shoulder peaks of W 4*f* have been reported in the electric-field-induced metallic phase of WO_3 [33]. Since the formal valence of W is +6, the origin of the metallic state is assigned to the charge transfer from O 2*p* to W 5*d* (effect of self-doping) by Altendorf *et al.* [33]. Most probably, the main and shoulder peaks in the metallic WO_3 can be assigned to the poorly and well-screened peaks due to the W 5*d* electrons induced by the self-doping.

The main and shoulder peaks of the W 4*f* spectra can be analyzed by fitting the spectra to five Lorentzian functions (one Lorentzian for W $5p_{3/2}$, and four Lorentzians for well- and poorly screened peaks of W $4f_{7/2}$ and W $4f_{5/2}$) and Shirley-type background. As shown in the middle and bottom panels of Fig. 4, the W 4*f* spectra can be decomposed into the well- and poorly screened peaks. At 300 K, the intensity ratio of the well-screened peak relative to the poorly screened peak is about 0.364. The intensity ratio of ∼0.4 is comparable to that of metallic $Ba_3Nb_5O_{15}$ [26,27]. However, it is still 0.360 at 180 K in the insulating phase. The only slight reduction may indicate that the W 5*d* electrons are still itinerant even in the insulating phase. This itinerancy of the W 5*d* electrons supports the Peierls scenario proposed by Streltsov *et al.* [10]. The energy separation between the well- and poorly screened peaks is about 1.65 eV at 300 K and about 1.71 eV at 180 K.

The fitted results in Fig. 4 could be affected by the large W 5*p* peak. Since the photoionization cross section of W 5*p* relative to that of W 4*f* becomes negligibly small in the soft x-ray region [17], W 4*f* spectra were also taken with photon energy of 1200 eV as shown in Fig. 5. Similar to the HAXPES results, the W $4f_{7/2}$ peak is accompanied by the shoulder structure on the lower binding energy side both at 240 and 190 K. However, the intensity of the shoulder peak is smaller with photon energy of 1200 eV than that with photon energy of 6.5 keV. Because of the reduced intensity, it is relatively difficult to fit the W 4*f* spectra to Lorentzian functions. By fixing the energy separation between the well- and poorly screened peaks to 1.6 eV, the W 4*f* spectra can be fitted to four Lorentzians as shown by the solid curves in Fig. 5. The intensity ratio of the well-screened peak relative to the poorly screened one is about 0.3 both at 240 and 190 K. The reduction of the well-screened peak in the surface sensitive SOXPES spectra may indicate that the number of W 5*d* electron is reduced in the surface region since SOXPES has a smaller probing depth than HAXPES.

In the valence-band HAXPES spectrum taken at 300 K, the W 5*d* peak is located around 0.4 eV as shown in Fig. 6. On the other hand, the W 5*d* peak is located around 0.8 eV at 300 K in the earlier study [12]. In the bulk sensitive HAXPES, the

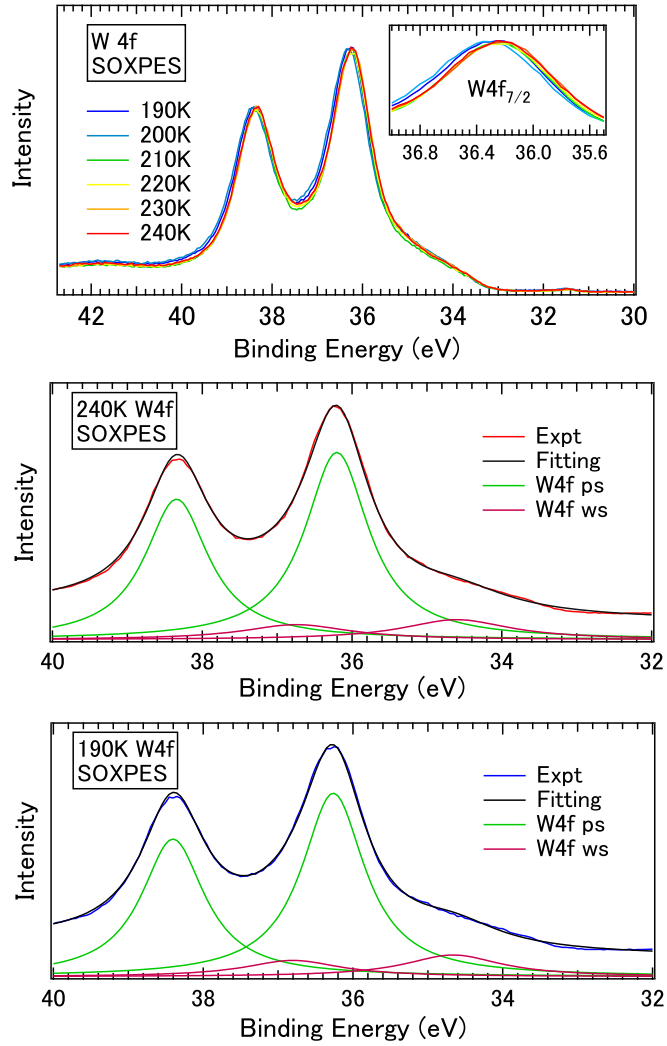

FIG. 5. W 4*f* SOXPES spectra of CsW_2O_6 taken at 240, 230, 220, 210, 200, and 190 K (top). The spectra at 240 K (middle) and 190 K (bottom) are fitted to Lorentzian functions. The solid curves represent the fitted results and the Lorentzian components.

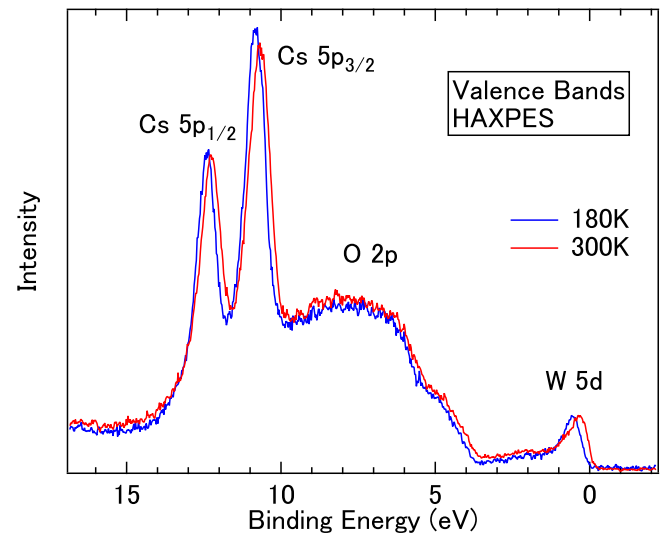

FIG. 6. Valence-band HAXPES spectra of CsW_2O_6 taken at 300 and 180 K.

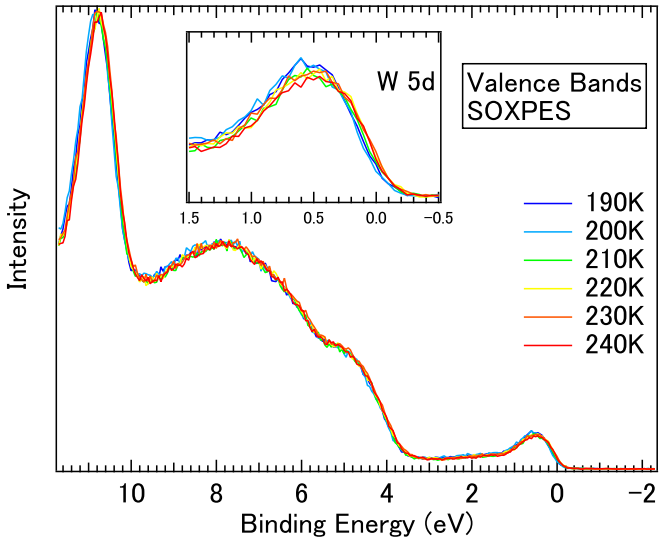

FIG. 7. Valence-band SOXPES spectra of CsW_2O_6 taken at 240, 230, 220, 210, 200, and 190 K.

W 5*d* band is rather narrow (width of about 1.2 eV) and is accompanied by a broad satellite peak around 2.0 eV. This is similar to the incoherent peak which is widely observed in various 3*d* [34–37] and 4*d* [26] electron systems. The O 2*p* band is observed around 4–10 eV below the Fermi level. The observed O 2*p* band is shifted toward higher binding energy from the calculated O 2*p* band [8]. In going from 300 to 180 K, the leading edge of the W 5*d* band is shifted by about 0.2 eV toward the higher binding energy side, indicating a band-gap opening of ∼0.2 eV at the Fermi level. The W 5*d* peak is located around 0.6 eV below the Fermi level at 180 K. The O 2*p* band and the Cs 5*p* levels are shifted by about 0.1 eV toward the higher binding energy side from 300 to 180 K. The energy shift of all the core levels including Cs 3*d* and 5*p* can be associated with the band-gap opening at the Fermi level. Here, it should be noted that the spectral weight of the O 2*p* band is mainly derived from the hybridized W 5*d* and Cs 5*p* components. The Cs 5*p* intensity is not negligible since the 5*p* photoionization cross section is extremely large at hard x-ray energies [38].

Figure 7 shows the valence-band SOXPES spectra at 240, 230, 220, 210, 200, and 190 K. The W 5*d* peak is located around 0.4–0.5 eV below the Fermi level in good agreement with the HAXPES results. The spectral weight at the Fermi level is reduced in going from 230 to 220 to 210 K, consistent with the metal-insulator transition of the bulk. Nevertheless, some spectral weight at the Fermi level remains even at 190 K. This observation may suggest that the surface region is still metallic even when the bulk becomes insulating. Most probably, the metal-insulator transition is disturbed at the surface region due to the decrease in the W 5*d* electrons as suggested by the W 4*f* spectra. Since the metal-insulator transition is driven by the trimerization due to the Peierls mechanism, the insulating phase would be destroyed by the reduction of the W 5*d* electron number.

IV. CONCLUSION

In conclusion, the electronic structure reconstruction across the metal-insulator transition of CsW_2O_6 has been studied by means of hard and soft x-ray photoelectron spectroscopy. In the high-temperature metallic phase, the W 5*d* band exhibits a clear Fermi edge indicating that the W 5*d* electrons are highly itinerant. However, the W $4f_{7/2}$ and $4f_{5/2}$ core-level peaks are accompanied by shoulders on their lower binding energy side. The main and shoulder peaks can be assigned to the poorly screened and well-screened peaks which are commonly observed in barely metallic or small gap 4*d* electron systems. The large intensity of the poorly screened peak suggests that the W 5*d* electrons are moderately correlated in CsW_2O_6. In going from 300 to 180 K (across the metal-insulator transition), the spectral weight of the well-screened peak is reduced but remains finite. In the valence-band spectra, the band gap of about 0.2 eV is created at the Fermi level at 180 K. The spectral changes and the opening of the band gap across the metal-insulator transition support the trimerization model of the W sites in CsW_2O_6. The W 4*f* and 5*d* spectra exclude a scenario involving charge disproportionation of the W ions.

ACKNOWLEDGMENTS

We acknowledge technical support from the staff of the MUSASHI beamline BL-2A of Photon Factory. The experiment at Photon Factory was performed with the approval of KEK (Proposal No. 2022G006). The HAXPES measurements were facilitated by the Max Planck-POSTECH-Hsinchu Center for Complex Phase Materials. This work was supported by Grants-in-Aid from the Japan Society of the Promotion of Science (JSPS) (Grant No. JP22H01172).

[1] S. Nagata, T. Hagino, Y. Seki, and T. Bitoh, Physica B **194-196**, 1077 (1994).
[2] M. Isobe and Y. Ueda, J. Phys. Soc. Jpn. **71**, 1848 (2002).
[3] P. G. Radaelli, Y. Horibe, M. J. Gutmann, H. Ishibashi, C. H. Chen, R. M. Ibberson, Y. Koyama, Y. S. Hor, V. Kirykhin, and S. W. Cheong, Nature (London) **416**, 155 (2002).
[4] M. Schmidt, W. Ratcliff, P. G. Radaelli, K. Refson, N. M. Harrison, and S. W. Cheong, Phys. Rev. Lett. **92**, 056402 (2004).
[5] D. I. Khomskii and T. Mizokawa, Phys. Rev. Lett. **94**, 156402 (2005).
[6] R. J. Cava, R. S. Roth, T. Siegrist, B. Hessen, J. J. Krajewski, and W. F. Peck, Jr., J. Solid State Chem. **103**, 359 (1993).
[7] D. Hirai, M. Bremholm, J. M. Allred, J. Krizan, L. M. Schoop, Q. Huang, J. Tao, and R. J. Cava, Phys. Rev. Lett. **110**, 166402 (2013).
[8] Y. Okamoto, H. Amano, N. Katayama, H. Sawa, K. Niki, R. Mitoka, H. Harima, T. Hasegawa, N. Ogita, Y. Tanaka, M. Takigawa, Y. Yokoyama, K. Takehana, Y. Imanaka, Y. Nakamura, H. Kishida, and K. Takenaka, Nat. Commun. **11**, 3144 (2020).
[9] K. Momma and F. Izumi, J. Appl. Crystallogr. **44**, 1272 (2011).

[10] S. V. Streltsov, I. I. Mazin, R. Heid, and K.-P. Bohnen, Phys. Rev. B **94**, 241101(R) (2016).
[11] H. Nakai and C. Hotta, Nat. Commun. **13**, 579 (2022).
[12] T. Soma, K. Yoshimatsu, K. Horiba, H. Kumigashira, and A. Ohtomo, Phys. Rev. Mater. **2**, 115003 (2018).
[13] Y. Okamoto, K. Niki, R. Mitoka, and K. Takenaka, J. Phys. Soc. Jpn. **89**, 124710 (2020).
[14] J. Weinen, T. C. Koethe, C. F. Chang, S. Agrestini, D. Kasinathan, Y. F. Liao, H. Fujiwara, C. Schler-Langeheine, F. Strigari, T. Haupricht, G. Panaccione, F. Offi, G. Monaco, S. Huotari, K.-D. Tsuei, and L. H. Tjeng, J. Electron Spectrosc. Relat. Phenom. **198**, 6 (2015).
[15] M. P. Seah and W. A. Dench, Surf. Interface Anal. **1**, 2 (1979).
[16] H. Shinotsuka, S. Tanuma, C. J. Powell, and D. R. Penn, Surf. Interface Anal. **51**, 427 (2019).
[17] J. J. Yeh and I. Lindau, At. Data Nucl. Data Tables **32**, 1 (1985).
[18] H.-D. Kim, H.-J. Noh, K. H. Kim, and S.-J. Oh, Physica B **359-361**, 1267 (2005).
[19] Z. V. Pchelkina, I. A. Nekrasov, T. Pruschke, A. Sekiyama, S. Suga, V. I. Anisimov, and D. Vollhardt, Phys. Rev. B **75**, 035122 (2007).
[20] G. Zhang and E. Pavarini, Phys. Rev. B **95**, 075145 (2017).
[21] A. Chikamatsu, Y. Kurauchi, K. Kawahara, T. Onozuka, M. Minohara, H. Kumigashira, E. Ikenaga, and T. Hasegawa, Phys. Rev. B **97**, 235101 (2018).
[22] T. T. Tran, K. Takubo, T. Mizokawa, W. Kobayashi, and I. Terasaki, Phys. Rev. B **73**, 193105 (2006).
[23] T. Sudayama, Y. Wakisaka, K. Takubo, T. Mizokawa, W. Kobayashi, I. Terasaki, S. Tanaka, Y. Maeno, M. Arita, H. Namatame, and M. Taniguchi, Phys. Rev. B **80**, 075113 (2009).
[24] D. Takegami, C.-Y. Kuo, K. Kasebayashi, J.-G. Kim, C. F. Chang, C. E. Liu, C. N. Wu, D. Kasinathan, S. G. Altendorf, K. Hoefer, F. Meneghin, A. Marino, Y. F. Liao, K. D. Tsuei, C. T. Chen, K.-T. Ko, A. Günther, S. G. Ebbinghaus, J. W. Seo, D. H. Lee, G. Ryu, A. C. Komarek, S. Sugano, Y. Shimakawa, A. Tanaka, T. Mizokawa, J. Kuneš, L. H. Tjeng, and A. Hariki, Phys. Rev. X **12**, 011017 (2022).
[25] Y. Nakatsu, A. Sekiyama, S. Imada, Y. Okamoto, S. Niitaka, H. Takagi, A. Higashiya, M. Yabashi, K. Tamasaku, T. Ishikawa, and S. Suga, Phys. Rev. B **83**, 115120 (2011).
[26] T. Yasuda, Y. Kondo, T. Kajita, K. Murota, D. Ootsuki, Y. Takagi, A. Yasui, N. L. Saini, T. Katsufuji, and T. Mizokawa, Phys. Rev. B **102**, 205133 (2020).
[27] R. Nakamura, T. Miyoshino, T. Kajita, T. Katsufuji, N. L. Saini, and T. Mizokawa, J. Phys. Soc. Jpn. **91**, 064711 (2022).
[28] M. Taguchi, A. Chainani, S. Ueda, M. Matsunami, Y. Ishida, R. Eguchi, S. Tsuda, Y. Takata, M. Yabashi, K. Tamasaku, Y. Nishino, T. Ishikawa, H. Daimon, S. Todo, H. Tanaka, M. Oura, Y. Senba, H. Ohashi, and S. Shin, Phys. Rev. Lett. **115**, 256405 (2015).
[29] T. Yoshino, M. Okawa, T. Kajita, S. Dash, R. Shimoyama, K. Takahashi, Y. Takahashi, R. Takayanagi, T. Saitoh, D. Ootsuki, T. Yoshida, E. Ikenaga, N. L. Saini, T. Katsufuji, and T. Mizokawa, Phys. Rev. B **95**, 075151 (2017).
[30] S. Dash, M. Okawa, T. Kajita, T. Yoshino, R. Shimoyama, K. Takahashi, Y. Takahashi, R. Takayanagi, T. Saitoh, D. Ootsuki, T. Yoshida, E. Ikenaga, N. L. Saini, T. Katsufuji, and T. Mizokawa, Phys. Rev. B **95**, 195116 (2017).
[31] S. Dash, T. Kajita, M. Okawa, T. Saitoh, E. Ikenaga, N. L. Saini, T. Katsufuji, and T. Mizokawa, Phys. Rev. B **97**, 165116 (2018).
[32] K. Takubo, S. Hirata, J.-Y. Son, J. W. Quilty, T. Mizokawa, N. Matsumoto, and S. Nagata, Phys. Rev. Lett. **95**, 246401 (2005).
[33] S. G. Altendorf, J. Jeong, D. Passarello, N. B. Aetukuri, M. G. Samant, and S. S. P. Parkin, Adv. Mater. **28**, 5284 (2016).
[34] K. Maiti, P. Mahadevan, and D. D. Sarma, Phys. Rev. Lett. **80**, 2885 (1998).
[35] K. Maiti, D. D. Sarma, M. J. Rozenberg, I. H. Inoue, H. Makino, O. Goto, M. Pedio, and R. Cimino, Europhys. Lett. **55**, 246 (2001).
[36] A. Sekiyama, H. Fujiwara, S. Imada, S. Suga, H. Eisaki, S. I. Uchida, K. Takegahara, H. Harima, Y. Saitoh, I. A. Nekrasov, G. Keller, D. E. Kondakov, A. V. Kozhevnikov, T. Pruschke, K. Held, D. Vollhardt, and V. I. Anisimov, Phys. Rev. Lett. **93**, 156402 (2004).
[37] R. J. O. Mossanek, M. Abbate, T. Yoshida, A. Fujimori, Y. Yoshida, N. Shirakawa, H. Eisaki, S. Kohno, P. T. Fonseca, and F. C. Vicentin, J. Phys.: Condens. Matter **22**, 095601 (2010).
[38] D. Takegami, L. Nicolaï, T. C. Koethe, D. Kasinathan, C. Y. Kuo, Y. F. Liao, K. D. Tsuei, G. Panaccione, F. Offi, G. Monaco, N. B. Brookes, J. Minár, and L. H. Tjeng, Phys. Rev. B **99**, 165101 (2019).